

Article

Design, Synthesis and Biological Evaluation of Novel Phenylsulfonylurea Derivatives as PI3K/mTOR Dual Inhibitors

Bingbing Zhao ¹, Fei Lei ¹, Caolin Wang ¹, Binliang Zhang ¹, Zunhua Yang ², Wei Li ³, Wufu Zhu ^{1,*}  and Shan Xu ^{1,*}

¹ School of Pharmacy, Jiangxi Science & Technology Normal University, Nanchang 330013, Jiangxi, China; zhaobb_0628@163.com (B.Z.); m13767032532@163.com (F.L.); wangcllw@163.com (C.W.); zbl1045762244@163.com (B.Z.)

² School of Pharmacy, Jiangxi University of Traditional Chinese Medicine, Nanchang 330004, Jiangxi, China; mtdzcool@163.com

³ School of Chemistry and Bioengineering, Yichun University, Yichun 336000, Jiangxi, China; nobel2025@163.com

* Correspondence: zhuwuf@jxstnu.edu.cn (W.Z.); xush@jxstnu.edu.cn (S.X.); Tel.: +86-791-8380-2393 (S.X.)

Received: 30 May 2018; Accepted: 19 June 2018; Published: 27 June 2018



Abstract: Five series of novel phenylsulfonylurea derivatives, **19a–d**, **20a–d**, **21a–d**, **22a–d** and **23a–d**, bearing 4-phenylaminoquinoline scaffold were designed, synthesized and their IC₅₀ values against four cancer cell lines (HepG-2, A549, PC-3 and MCF-7) were evaluated. Most compounds showed moderate cytotoxicity activity against the cancer cell lines. Structure–activity relationships (SARs) and pharmacological results indicated that introduction of 4-aminoquinoline scaffold and phenylsulfonylurea scaffold were beneficial for anti-tumor activity. Moreover, para-methoxy substitution of 4-anilino moiety and para-halogen substitution of phenylsulfonylurea have different impacts on different series of compounds. Furthermore, the micromolecule group substitution in the 6-position of the quinoline ring have a slight impact on the cellular activity of the target compounds.

Keywords: 4-phenylaminoquinoline; phenylsulfonylurea; PI3K/mTOR; inhibitor

1. Introduction

PI3K (phosphatidylinositol-3-kinase) is a kind of cellular signaling molecule, which is closely associated with human cancers. According to the primary structures, regulatory mechanisms and distribution positions, the PI3K families [1–3] are divided into four different types: Type I, Type II, Type III and Type IV. The type I PI3K enzymes are further divided into PI3K α , PI3K β , PI3K δ and PI3K γ [4,5]. PI3K/mTOR signaling pathway plays a crucial role in regulating various cellular physiological activities such as proliferation, growth, proliferation and apoptosis [6]. With the development of cytobiology, accumulating studies have shown that the PI3K/mTOR signaling pathway is frequently disregarded in most tumor cells, leading to malignant proliferation of normal organism cells [7–9]. In addition, research has also shown that PI3K/mTOR signaling pathway can promote the occurrence of cancer by promoting angiogenesis, accelerating cell growth cycle and promoting tumor cell metastasis [10]. Therefore, the development of double inhibitors targeting PI3K/mTOR has become a hotspot in this field. Thus far, numerous PI3K/mTOR double target inhibitors have been developed into clinical trial, such as NVPBEZ235 [11], GSK2126458 [12], GDC0980 [13], PKI587 [14], BGT226 [15] and PF06491502 [16] (Figure 1). Furthermore, most of these compounds shared quinoline core and exhibited remarkable potency in both enzymatic and cellular inhibitory activity [17]. Research

data further demonstrated that PI3K/mTOR double target inhibitors have a great potential in the process of anti-tumor therapy [18,19].

4-Amino quinazoline derivatives have been widely used in small molecule antitumor drugs for their multiple biological activities, especially EGFR inhibitors [17]. Compounds containing 4-amino quinazoline core account for a substantial proportion of therapeutic drugs [20], such as Gefitinib, Erlotinib, Afatinib and Vandetanib. The potency of these drugs has been widely recognized in clinical treatment. Accordingly, we introduced 4-amino quinazoline structure into PI3K/mTOR inhibitor to investigate antiproliferative activity of 4-amino quinazoline structure on tumor cells.

We firstly introduced 4-aminoquinoline structure by ring-opening the imidazolone structure of NVPBEZ235. To guide our design, we carried out the molecular simulation to find the differences between the binding mode of GSK2126458 and NVPBEZ235 with PI3K γ protein. From the docking results in Figure 2, we can see that both drugs can form the hydrogen bond between the N-atom in quinoline rings and valine. The -CN of substituted aniline side chain in the NVPBEZ235 points to the hydrophobic cavity and forms a hydrogen bond with SER806. This suggests that the para position of 4-aniline side chain is a key active site. Therefore, we introduced electron-withdrawing group -Br, electron-donating group -OCH₃, 3-Cl-4-F-aniline active group, 4-Br-2-F-aniline active group and retained -CN to change benzene ring electron cloud density. Through this design strategy, we expect to obtain desirable inhibitors with better PI3K/mTOR inhibition activity. In addition, benzene sulfonamide structure of GSK2126458 buried into hydrophobic pockets, and the O-atom of sulfonyl group formed a hydrogen bond with residue LYS833. Therefore, we secondly introduced benzene sulfonamide group into NVPBEZ235 to explore potential interactions between the PI3K γ protein and target compounds, and also improve the water solubility. Based on the above, we used the same design strategy to introduce different substituent groups into the para-position of phenylsulfonamide. On the one hand, we changed the electron cloud density of benzene ring. On the other hand, we appropriately increased the space structure of benzene ring to enhance the affinity of small molecule ligand with receptor protein. Finally, series of 4-aniline quinoline derivatives containing phenylsulfonamide structure were designed, synthesized and all compounds were evaluated for their anti-proliferative effects.

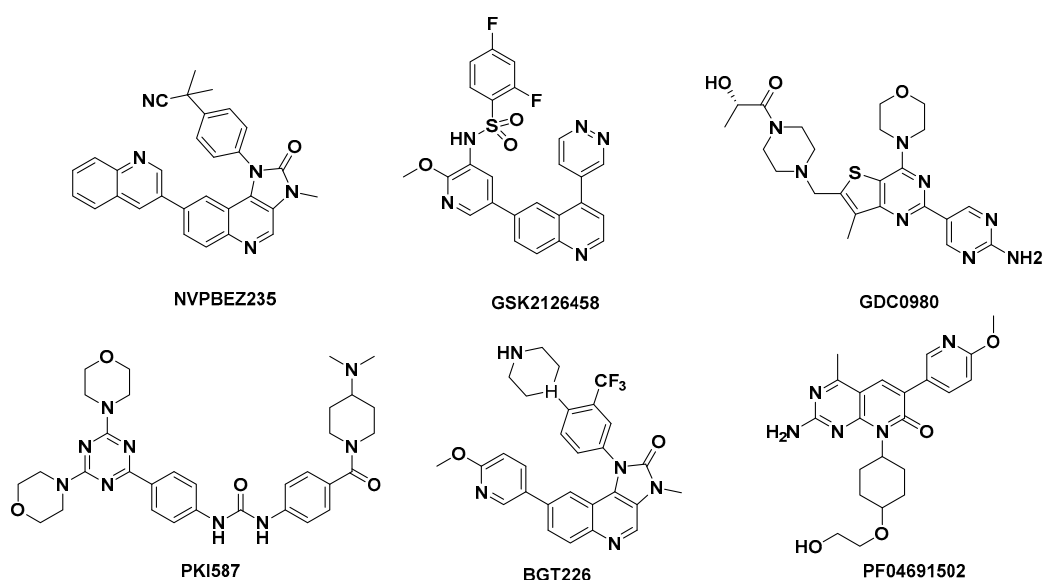


Figure 1. Structures of representative clinical PI3K/mTOR dual inhibitors.

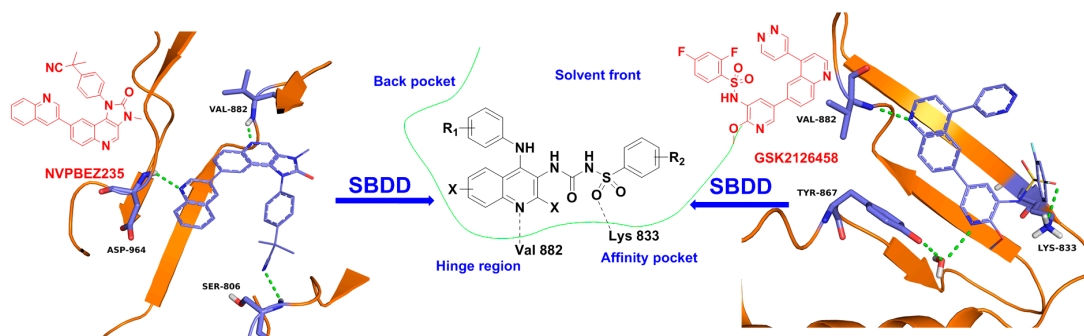
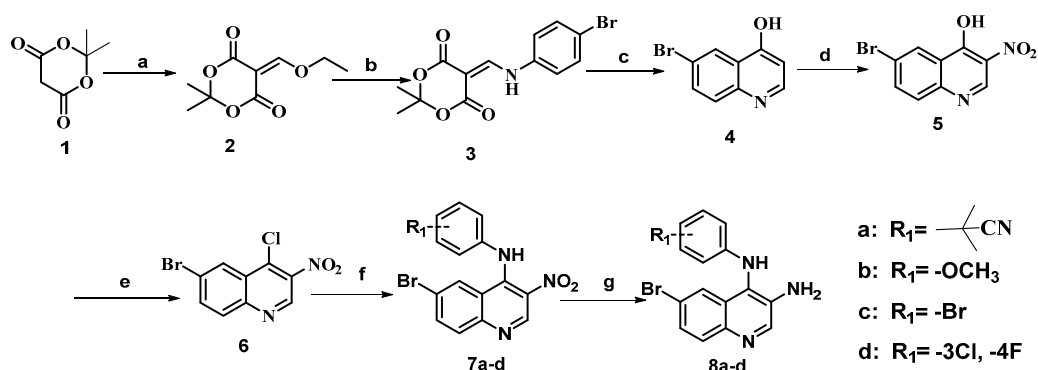


Figure 2. Structure based drug design strategy based on the molecular simulation.

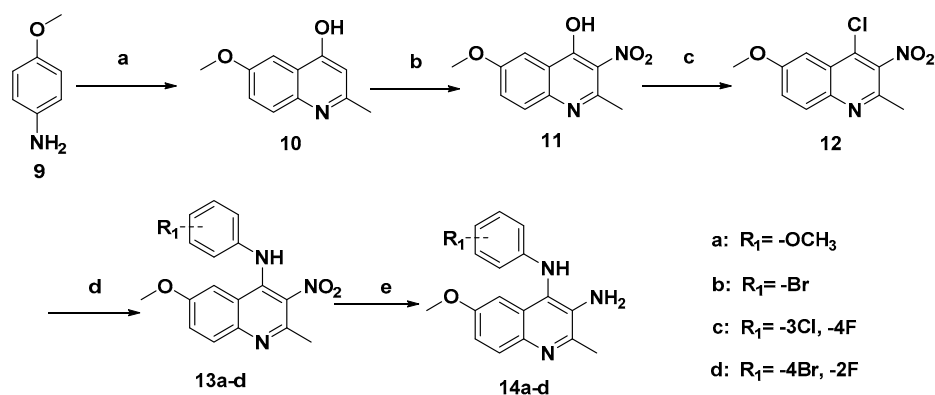
2. Results and Discussion

2.1. Chemistry

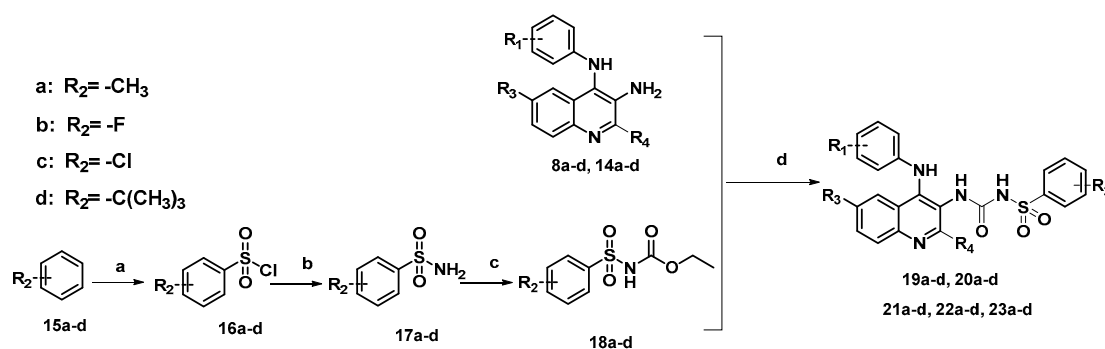
Based on the structure based drug design (SBDD) strategy, taking NVPBEZ235 as reference compound, five series of PI3K/mTOR inhibitors were designed and synthesized. The synthetic routes of target compounds 19a–d, 20a–d, 21a–d, 22a–d and 23a–d are outlined in Schemes 1–3.



Scheme 1. The synthetic route for target compounds 8a–d. Reagents and conditions: (a) Triethoxy methane; (b) 4-Bromoanilines, C_2H_5OH , reflux, $105\text{ }^\circ\text{C}$, 6 h; (c) Ph_2O , $200\text{ }^\circ\text{C}$, Microwave, 15 min; (d) HNO_3 , Propionic acid, $125\text{ }^\circ\text{C}$, 2 h; (e) $POCl_3$, DMF, $100\text{ }^\circ\text{C}$, 3 h; (f) Substituted aniline, Acetic acid, $100\text{ }^\circ\text{C}$, 5 h; and (g) $FeCl_3$, $N_2H_4 \cdot H_2O$, C_2H_5OH , $80\text{ }^\circ\text{C}$, 3 h.



Scheme 2. The synthetic route for target compounds 13a–d. Reagents and conditions: (a) PPA, $190\text{ }^\circ\text{C}$, 6 h; (b) HNO_3 , Propionic acid, $125\text{ }^\circ\text{C}$, 2 h; (c) $POCl_3$, DMF, $100\text{ }^\circ\text{C}$, 3 h; (d) Substituted aniline, Acetic acid, $100\text{ }^\circ\text{C}$, 5 h; and (e) $FeCl_3$, $N_2H_4 \cdot H_2O$, C_2H_5OH , $80\text{ }^\circ\text{C}$, 3 h.

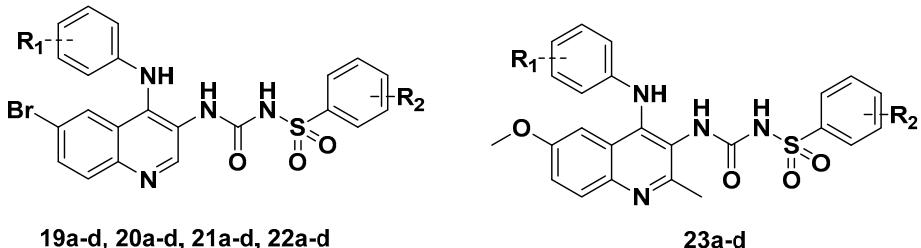


Scheme 3. The synthetic route for target compounds **19a–d**, **20a–d**, **21a–d**, **22a–d** and **23a–d**. Reagents and conditions: (a) HSO_3Cl , reflux, 6 h; (b) C_2H_5OH , $0^\circ C$, 1 h; (c) DIPEA, CH_2Cl_2 , r.t., 0.5 h; and (d) Toluene, $120^\circ C$, 6 h.

As shown in Schemes 1–3, all target compounds were synthesized by resolution synthetic method. Target compounds were separately split into 4-anilinoquinoline fragment in the left half and phenylsulfonylurea fragment in the right half, and finally the two fragments were connected to obtain target compounds. As shown in Scheme 1, we used commercially available isopropyl malonate (**1**) and triethyl orthoformate as starting materials to obtain segments **8a–d** by seven steps of condensation, cyclization, substitution, nitration, chlorination, amination and reduction. Then, we used **9** as the starting material to get fragments **14a–d** by a method similar to that of synthesizing **8a–d**. Detailed synthetic route of **14a–d** is shown in Scheme 2. Next, as shown in Scheme 3, we used different substituted aromatic rings as starting materials to obtain fragments **18a–d** by chlorosulfonation, aminolysis and substitution reaction. Finally, target compounds **19a–d**, **20a–d**, **21a–d**, **22a–d** and **23a–d** were obtained by linking fragments **18a–d** with fragments **8a–d** and **14a–d**, respectively. The structural information of all target compounds was confirmed by 1H -NMR, ^{13}C -NMR and TOF MS (ES+), which were in agreement with the structures depicted.

2.2. Biological Discussion

Four cells (HepG-2, A549, PC-3, MCF-7) were selected to evaluate the in vitro antiproliferative activity of all target compounds. As shown in Table 1, phenylsulfonylurea derivatives (**19a–d**, **20a–d**, **21a–d** and **22a–d**) with bromine substitution at 6-position of quinoline ring showed moderate antiproliferative activity against HepG-2 cell, A549 cell and PC-3 cell, and some compounds (**19a** and **19c**) showed strong sensitivity to MCF-7 cell. In addition, the introduction of different substituents into 4-position of aniline in the quinoline ring can significantly improve anti-proliferative activity and cell selectivity of target compounds, and when aniline was substituted with $-CN$ or $-OCH_3$, target compounds (**19a–d** and **20a–d**) showed stronger anti-proliferative activity to MCF-7 cell. Compounds with $-CN$ or $-OCH_3$ substituted at the 4-position of aniline structure in the quinoline ring showed better anti-proliferative activity against MCF-7 cell than that of the other three cells. When $-CH_3$ or $-Cl$ -atom were introduced into the phenylsulfonylurea structure, target compounds (**20c** and **22b**) showed good anti-proliferative activity on MCF-7 cell, but when aniline was substituted with F -atom or Cl -atom, the anti-proliferative activity of target compound (**21a–d**) on MCF-7 cell was weaker than that of other three cells. Overall, 4-anilino side chain para-methoxy substituted compounds **20a–d** showed better MCF-7 cell anti-proliferation activity than other compounds (**19a–d**, **21a–d** and **22a–d**). We speculate that electron-donating group $-OCH_3$ increased the electron cloud density of aniline side chain. Thus, the force between aniline side chain and hydrophobic cavity of protein was enhanced.

Table 1. Structures and cytotoxicity of compounds **19a–d**, **20a–d**, **21a–d**, **22a–d** and **23a–d**.


Compound	R ₁	R ₂	IC ₅₀ (μM) ^a			
			HepG-2	A549	PC-3	MCF-7
19a	pivalonitrile	-F	33.28 ± 1.52	38.52 ± 1.04	66.62 ± 1.28	3.88 ± 0.58
19b	pivalonitrile	-Cl	30.22 ± 1.45	>100	34.31 ± 1.32	15.10 ± 1.1
19c	pivalonitrile	-CH ₃	31.25 ± 1.50	28.96 ± 1.31	40.59 ± 1.11	3.96 ± 0.59
19d	pivalonitrile	Tert-Butyl	>100	30.58 ± 1.45	68.25 ± 1.32	9.95 ± 0.99
20a	-OCH ₃	-F	20.34 ± 1.04	26.34 ± 1.13	>100	7.65 ± 0.88
20b	-OCH ₃	-Cl	22.56 ± 1.12	30.22 ± 1.23	>100	10.65 ± 0.97
20c	-OCH ₃	-CH ₃	26.83 ± 1.22	23.35 ± 1.12	>100	4.94 ± 0.64
20d	-OCH ₃	Tert-Butyl	33.24 ± 1.26	32.12 ± 1.18	>100	10.46 ± 0.98
21a	-Br	-F	45.68 ± 1.66	58.98 ± 1.76	>100	37.59 ± 1.57
21b	-Br	-Cl	11.13 ± 1.04	71.11 ± 1.85	>100	13.78 ± 1.14
21c	-Br	-CH ₃	31.05 ± 1.49	22.74 ± 1.35	>100	16.63 ± 1.22
21d	-Br	Tert-Butyl	16.97 ± 1.22	16.16 ± 1.20	>100	52.67 ± 1.72
22a	-3-Cl-4-F	-F	19.63 ± 0.18	12.02 ± 0.91	52.52 ± 1.03	22.83 ± 1.35
22b	-3-Cl-4-F	-Cl	6.443 ± 0.89	>100	17.72 ± 0.95	6.84 ± 0.83
22c	-3-Cl-4-F	-CH ₃	11.274 ± 0.84	>100	16.74 ± 0.88	16.81 ± 1.22
22d	-3-Cl-4-F	Tert-Butyl	28.43 ± 0.89	22.40 ± 1.21	29.27 ± 2.23	46.30 ± 1.67
23a	-OCH ₃	-Cl	15.98 ± 1.10	39.76 ± 1.59	>100	6.30 ± 0.79
23b	-OCH ₃	Tert-Butyl	2.71 ± 0.43	7.47 ± 0.87	>100	6.55 ± 0.81
23c	-Br	-F	32.12 ± 1.12	12.96 ± 0.84	39.76 ± 1.25	25.44 ± 1.43
23d	-3-Cl-4-F	-F	6.08 ± 1.04	38.14 ± 0.96	57.85 ± 0.99	57.03 ± 1.75
NVP-BEZ235 ^b	-	-	0.54 ± 0.83	0.36 ± 0.86	0.20 ± 0.11	0.14 ± 0.10
Sorafenib ^b	-	-	3.97 ± 0.13	6.53 ± 0.23	3.03 ± 0.11	4.21 ± 0.15

^a The values are an average of two separate determinations; ^b used as a positive control.

Phenylsulfonylurea derivatives (**23a–d**) with methoxyl substitution at 6-position of the quinoline ring showed moderate antitumor activity against HepG-2 cell, A549 cell and PC-3 cell. Similarly, 4-anilino side chain para-methoxy substituted compounds **23a** and **23b** showed better MCF-7 cell anti-proliferation activity than that of other compounds (**23c** and **23d**). It is noteworthy that the activity of compounds **23a–d** to HepG-2 cell was generally superior to that of the other three cells, especially compounds **23b** and **23d** (with an IC₅₀ value of 2.71 μM and 6.08 μM, respectively). We supposed that the quinoline ring and the 4-phenylamino side chain of compound **23b** are not only both located in the hydrophobic cavity of the protein but also all substituted by electron-donating group -OCH₃ group, which greatly increased the electron cloud density of the structure in the left half of compound **23b**. Thus, the affinity between compound **23b** and the target protein was enhanced. In addition, from the docking results (Figure 3), we can see that the -OCH₃ group on the quinoline ring of compound **23b** points to inside of the protein cavity and fully occupies the space of this part, thus resulting in better antiproliferative activity of compounds **23a–d** against HepG-2 cell.

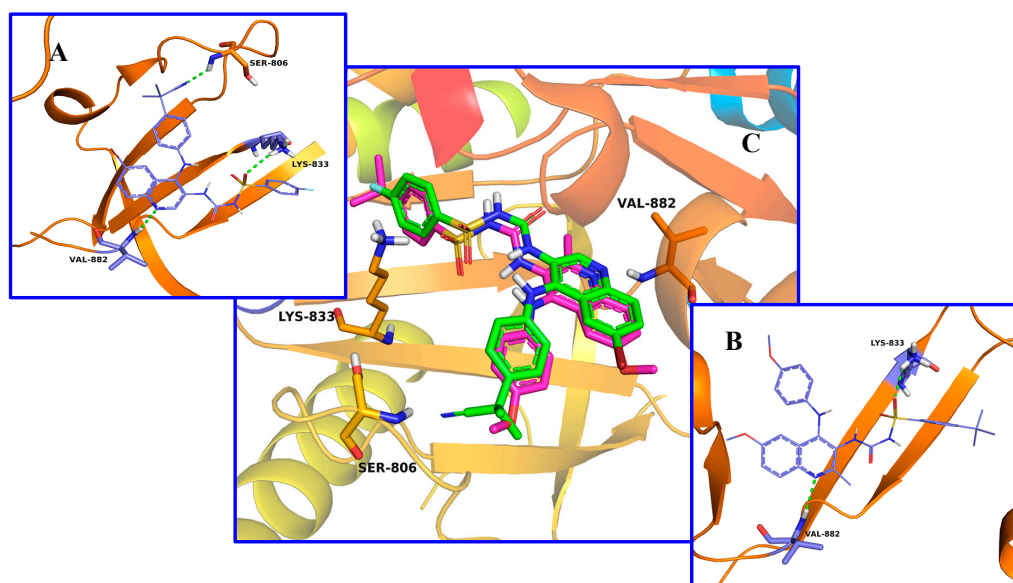


Figure 3. (A) The binding mode of compound **19a** with PI3K γ (3L08) kinase; (B) the binding mode of compound **23b** with PI3K γ kinase; and (C) the contrast of binding mode between compound **19a** (green) and **23b** (red).

Finally, the inhibitory rate against PI3K α kinase and mTOR kinase of selected compounds **19a** and **23b** at 10 μ M was further examined. As shown in Table 2, enzymatic activity results of compounds **19a** and **23b** exhibited a moderate inhibitory rate against PI3K α kinase and mTOR kinase.

Table 2. Enzymatic activities of compounds **19a** and **23b** against PI3K α and mTOR (IC₅₀, μ M).

Compound	IC ₅₀ (μ M)	
	PI3K α	mTOR
19a	0.72	2.62
23b	>10	>10
NVP-BEZ235	0.004 \pm 0.002	0.006 \pm 0.003
PI101	0.011 \pm 0.002	0.019 \pm 0.002

PI3K α : Phosphatidylinositol-3-kinase alpha subunit; mTOR: Mammalian target of rapamycin.

2.3. Molecular Docking Study

To explore the binding modes of target compounds (**19a** and **23b**) with the active site of PI3K γ , molecular docking simulation studies were carried out by the AutoDock 4.2 software. The docking tutorial we used and the detailed AutoDock basic operational methods can be found at: <http://autodock.scripps.edu/faqs-help/tutorial>. Based on in vitro inhibition results, we selected compounds **19a** and **23b** as ligand examples, and the structures of PI3K γ (PDB code: 3L08) were selected as the docking models. Only the best-scoring ligand–protein complex (Figure 3) was used for the binding site analysis.

The binding mode of compounds **19a** and **23b** with the active site of PI3K γ molecular is shown in Figure 3, which depicts that the oxygen atom on benzene sulfonamide group of compounds **19a** and **23b** both formed a hydrogen bond with PI3K γ residue LYS833 and the nitrogen atom in quinoline ring formed a hydrogen bond with hinge residue VAL882. In the docking model of compound **19a** with PI3K γ , we can see the cyano group on the aniline group in the 4-position of quinoline ring formed a hydrogen bond with the residue SER806. All these factors above contribute to the excellent antiproliferative activity and selectivity of the compound **19a**. The whole 4-aminoquinoline ring

structure of the selected compounds extended into ATP hydrophobic pocket, which is basically the same as our previous prediction binding mode (shown in Figure 2). Furthermore, binding modes of compounds **19a** and **23b** were almost completely overlapped. The abovementioned SAR (Structure–Activity Relationship) analysis and molecular docking study results may allow the rational design of potential PI3K and mTOR inhibitors.

3. Experimental Section

3.1. General Information

Unless otherwise required, all reagents used in the experiment were purchased as commercial analytical grade and used without further purification. Frequently used solvents (Ethanol, petroleum ether, ethyl acetate, dichloromethane, etc.) were absolutely anhydrous. All actions were monitored through GF₂₅₄ thin-layer chromatography plate and spots were visualized with iodine or light (in 254 nm or 365 nm). The structure of the target compound was confirmed by ¹H-NMR and ¹³C-NMR spectra at room temperature on Bruker 400 MHz spectrometer (Bruker Bioscience, Billerica, MA, USA) with tetramethylsilane (TMS) as an internal standard. Mass spectrometry (MS) was performed on Waters High Resolution Quadrupole Time of Flight Tandem Mass Spectrometry (QTOF). The purity of the compound was determined by Agilent 1260 liquid chromatograph fitted with an Inertex-C18 column. All target compounds had the purity of ≥95%.

3.2. Chemistry

3.2.1. General Procedure for the Preparation of Compounds **8a–d**, **14a–d** and **18a–d**

We used isopropyl malonate (**1**) and triethyl orthoformate as the starting material to get intermediate **2**. Next, intermediate **2** was condensed and cyclized with *p*-bromoaniline to obtain 4-hydroxy-6-bromoquinoline (**5**), and then 3-nitro-4-chloro-6-bromoquinoline (**6**) was generated by nitration and chlorination. Intermediate **6** reacted with para-substituted anilines (**a–d**) to obtain intermediates **7a–d**, and then underwent a reduction reaction to obtain intermediates **8a–d**. Similarly, we used 4-methoxyaniline (**9**) as the starting material to obtain intermediates **14a–d** through a similar reaction. Chlorosulfonic acid was reacted with different substituted anilines (**15a–d**) to obtain (**16a–d**), and then **18a–d** were obtained by amination reaction and acylation reaction.

3.2.2. General Procedure for Preparation of Target Compounds **19a–d**, **20a–d**, **21a–d**, **22a–d** and **23a–d**

A solution of ethyl (phenylsulfonyl) carbamate (1.2 mmol, **18a–d**) in toluene (5 mL) was added dropwise to a solution of **8a–d** or **14a–d** (1 mmol) in toluene (15 mL). Upon completion of the addition, the reaction mixture was stirred at 120 °C for 6 h and monitored by thin-layer chromatography (TLC). The reaction mixture was cooled to room temperature and concentrated under a reduced pressure. Then, ethyl acetate was added and the insoluble materials were collected by filtration and dried to yield the target compounds **19a–d**, **20a–d**, **21a–d**, **22a–d** and **23a–d**, which were recrystallized from isopropanol.

N-((6-Bromo-4-((4-(2-cyanopropan-2-yl)phenyl)amino)quinolin-3-yl)carbamoyl)-4-fluorobenzenesulfonamide carboxamide (**19a**). A pale white solid; Yield: 52.6%; m.p.: 315.2–316.4 °C; ¹H-NMR (400 MHz, DMSO-*d*₆) δ (ppm): 12.01 (s, 1H), 8.95 (s, 1H), 8.08 (d, *J* = 9.0 Hz, 1H), 8.05–7.94 (m, 4H), 7.82 (dd, *J* = 16.8, 8.6 Hz, 3H), 7.59–7.50 (m, 3H), 7.11 (s, 1H), 1.95 (s, 6H). ¹³C NMR (400 MHz, DMSO-*d*₆) δ 165.41, 153.89, 143.83, 142.85, 134.90, 132.57, 130.12, 129.89 × 2, 129.42, 129.06, 128.97, 127.26 × 2, 124.80, 122.84, 122.66, 119.37, 116.55 × 2, 116.40, 116.33 × 2, 37.32, 28.86 × 2. TOF MS ES⁺ (*m/z*): [M + H]⁺, calcd for C₂₆H₂₁BrFN₅O₃S: 581.0533, found: 582.0611.

N-((6-Bromo-4-((4-(2-cyanopropan-2-yl)phenyl)amino)quinolin-3-yl)carbamoyl)-4-chlorobenzenesulfonamide (**19b**). A pale white solid; Yield: 50.1%; m.p.: 279.2–280.1 °C; ¹H-NMR (400 MHz, DMSO-*d*₆) δ (ppm):

11.87 (s, 1H), 8.81 (s, 1H), 8.23(d, $J = 9.8$ Hz, 2H), 7.94 (d, $J = 9.0$ Hz, 1H), 7.89 (s, 1H), 7.88 (d, $J = 3.1$ Hz, 1H), 7.85 (s, 1H), 7.83 (s, 1H), 7.70 (d, $J = 8.2$ Hz, 2H), 7.66 (d, $J = 9.1$ Hz, 1H), 7.45–7.38 (m, 3H), 6.97 (s, 1H), 1.81 (s, 6H), ^{13}C -NMR (400 MHz, DMSO- d_6) δ 153.88, 143.79, 143.12, 135.17 \times 2, 134.93, 132.86 \times 2, 129.95, 129.90 \times 2, 129.15, 127.24 \times 2, 126.09, 124.80, 122.83, 122.62 \times 2, 122.62, 119.30, 116.45, 102.00, 37.32, 28.86 \times 2, 21.37. TOF MS ES⁺ (m/z): [M + H]⁺, calcd for C₂₆H₂₁BrClN₅O₃S: 597.0237, found: 598.0315.

N-((6-Bromo-4-((4-(2-cyanopropan-2-yl)phenyl)amino)quinolin-3-yl)carbamoyl)-4-methylbenzenesulfonamide (**19c**). A pale white solid; Yield: 51.4%; m.p.: 289.2–290.4 °C; ^1H -NMR (400 MHz, DMSO- d_6) δ (ppm): 12.01 (s, 1H), 8.95 (s, 1H), 8.25(d, $J = 9.5$ Hz), 8.08 (d, $J = 9.0$ Hz, 1H), 7.98 (d, $J = 8.4$ Hz, 3H), 7.84 (d, $J = 8.2$ Hz, 2H), 7.80 (d, $J = 9.1$ Hz, 1H), 7.59–7.51 (m, 3H), 7.11 (s, 1H), 6.23 (s, 1H), 2.30 (s, 3H) 1.95 (s, 6H). ^{13}C -NMR (400 MHz, DMSO- d_6) δ 153.88, 143.79, 143.12, 135.17 \times 2, 134.93, 132.86 \times 2, 129.95, 129.90 \times 2, 129.15, 127.24 \times 2, 126.09, 124.80, 122.83, 122.62 \times 2, 122.62, 119.30, 116.45, 102.00, 37.32, 28.86 \times 2, 21.37. TOF MS ES⁺ (m/z): [M + H]⁺, calcd for C₂₇H₂₄BrN₅O₃S: 577.0783, found: 578.0861.

N-((6-Bromo-4-((4-(2-cyanopropan-2-yl)phenyl)amino)quinolin-3-yl)carbamoyl)-4-(*tert*-butyl)benzenesulfonamide (**19d**). A pale white solid; Yield: 45.6%; m.p.: 287.2–288.4 °C; ^1H -NMR (400 MHz, DMSO- d_6) δ (ppm): 12.06 (s, 1H), 9.00 (s, 1H), 8.23 (s, 1H), 8.13 (d, $J = 9.0$ Hz, 1H), 8.03 (d, $J = 8.4$ Hz, 4H), 7.89 (d, $J = 8.2$ Hz, 2H), 7.85 (d, $J = 9.1$ Hz, 1H), 7.65–7.57 (m, 3H), 7.16 (s, 1H), 2.00 (s, 1H), 1.63 (s, 9H), ^{13}C -NMR (400 MHz, DMSO- d_6) δ 156.15, 153.88, 143.77, 143.09, 135.17, 134.91, 132.87, 129.96, 129.92, 128.97 \times 3, 127.25 \times 2, 125.32 \times 2, 121.18, 121.09, 120.15 \times 2, 119.72, 118.38, 116.44, 37.32, 29.72, 28.84 \times 3, 25.62 \times 2. TOF MS ES⁺ (m/z): [M + H]⁺, calcd for C₃₀H₃₀BrN₅O₃S: 619.1253, found: 620.1331.

N-((6-Bromo-4-((4-methoxyphenyl)amino)quinolin-3-yl)carbamoyl)-4-fluorobenzenesulfonamide (**20a**). A pale white solid; Yield: 47.9%; m.p.: 289.1–290.2 °C; ^1H -NMR (400 MHz, DMSO- d_6) δ (ppm): 11.93 (s, 1H), 8.93 (s, 1H), 8.08 (d, $J = 9.0$ Hz, 1H), 7.86 (d, $J = 8.0$ Hz, 2H), 7.82–7.77 (d, $J = 8.6$ Hz, 1H), 7.68 (d, $J = 8.7$ Hz, 2H), 7.52 (d, $J = 8.0$ Hz, 2H), 7.43 (s, 2H), 7.37 (d, $J = 8.7$ Hz, 2H), 7.28 (s, 1H), 4.05 (s, 3H), ^{13}C -NMR (400 MHz, DMSO- d_6) δ 165.72, 153.88, 152.52, 143.78, 138.17, 136.91, 132.86, 130.98 \times 2, 129.92, 128.81, 128.26, 121.98, 121.61 \times 2, 119.57, 118.32, 117.44, 116.02 \times 2, 115.18 \times 2, 59.84. TOF MS ES⁺ (m/z): [M + H]⁺, calcd for C₂₃H₁₈BrFN₄O₄S: 544.0216, found: 545.0294.

N-((6-Bromo-4-((4-methoxyphenyl)amino)quinolin-3-yl)carbamoyl)-4-chlorobenzenesulfonamide (**20b**). A pale white solid; Yield: 48.2%; m.p.: 282.2–283.1 °C; ^1H -NMR (400 MHz, DMSO- d_6) δ (ppm): 10.83 (s, 1H), 8.87 (s, 1H), 8.68 (s, 1H), 8.48 (s, 1H), 8.08–7.89 (d, $J = 8.0$ Hz, 2H), 7.84 (d, $J = 8.0$ Hz, 2H), 7.58 (d, $J = 8.7$ Hz, 2H), 7.51 (d, $J = 8.0$ Hz, 2H), 7.43 (s, 2H), 7.37 (d, $J = 8.7$ Hz, 2H), 7.07 (s, 1H), 3.97 (s, 3H), ^{13}C -NMR (400 MHz, DMSO- d_6) δ 153.72, 153.03, 144.05, 138.95, 138.47, 137.41, 132.86, 130.03 \times 3, 128.92 \times 2, 128.81, 128.02, 121.88, 121.76 \times 2, 119.86, 118.91, 117.84, 115.11 \times 2, 59.64. TOF MS ES⁺ (m/z): [M + H]⁺, calcd for C₂₃H₁₈BrClN₄O₄S: 559.9921, found: 560.9999.

N-((6-Bromo-4-((4-methoxyphenyl)amino)quinolin-3-yl)carbamoyl)-4-methylbenzenesulfonamide (**20c**). A pale white solid; Yield: 46.6%; m.p.: 279.2–280.6 °C; ^1H -NMR (400 MHz, DMSO- d_6) δ (ppm): 11.77 (s, 1H), 8.77 (s, 1H), 7.93 (d, $J = 9.0$ Hz, 1H), 7.70 (d, $J = 8.0$ Hz, 2H), 7.67–7.60 (m, 1H), 7.53 (d, $J = 8.7$ Hz, 2H), 7.36 (d, $J = 8.0$ Hz, 2H), 7.28 (s, 2H), 7.21 (d, $J = 8.7$ Hz, 2H), 7.13 (s, 1H), 3.89 (s, 3H), 2.37 (s, 3H). ^{13}C -NMR (400 MHz, DMSO- d_6) δ 160.46, 154.20, 143.08, 142.33, 141.89, 135.04, 132.80, 130.57 \times 2, 129.91, 129.77, 129.49 \times 2, 127.81, 126.08 \times 2, 122.63, 122.59, 119.24, 116.57, 115.52 \times 2, 56.13, 21.38. TOF MS ES⁺ (m/z): [M + H]⁺, calcd for C₂₄H₂₁BrN₄O₄S: 540.0467, found: 541.0545.

N-((6-Bromo-4-((4-methoxyphenyl)amino)quinolin-3-yl)carbamoyl)-4-(*tert*-butyl)benzenesulfonamide (**20d**). A pale white solid; Yield: 40.6%; m.p.: 263.3–264.2 °C; ^1H -NMR (400 MHz, DMSO- d_6) δ (ppm): 11.93 (s, 1H), 8.93 (s, 1H), 8.08 (d, $J = 9.0$ Hz, 1H), 7.86 (d, $J = 8.0$ Hz, 2H), 7.82–7.77 (d, $J = 8.6$ Hz, 1H), 7.68 (d, $J = 8.7$ Hz, 2H), 7.52 (d, $J = 8.0$ Hz, 2H), 7.43 (s, 2H), 7.37 (d, $J = 8.7$ Hz, 2H), 7.28 (s, 1H), 4.05 (s, 3H), 1.72 (s, 9H), ^{13}C -NMR (400 MHz, DMSO- d_6) δ 154.87, 153.23, 152.12, 143.27, 138.54, 137.24, 132.48, 129.45, 128.36, 128.97 \times 2, 129.87, 125.32 \times 2, 121.89, 121.43 \times 2, 119.58, 118.65, 118.47, 115.52 \times

2, 55.98, 35.12, 31.25 × 3. TOF MS ES⁺ (*m/z*): [M + H]⁺, calcd for C₂₇H₂₇BrN₄O₄S: 582.0936, found: 583.1015.

N-((6-Bromo-4-((4-bromophenyl)amino)quinolin-3-yl)carbamoyl)-4-fluorobenzenesulfonamide (**21a**). A pale white solid; Yield: 45.8%; m.p.: 278.7–279.5 °C; ¹H-NMR (400 MHz, DMSO-*d*₆) δ (ppm): 12.04 (s, 1H), 8.95 (s, 1H), 8.84 (s, 2H), 8.76 (s, 1H), 8.34 (d, *J* = 12.0 Hz, 4H), 8.19 (s, 1H), 7.76 (d, *J* = 8.5 Hz, 2H), 7.42 (d, *J* = 8.5 Hz, 2H), 6.60 (s, 1H). ¹³C-NMR (400 MHz, DMSO-*d*₆) δ 144.98, 138.52, 135.18, 133.35, 131.99, 131.92, 131.73, 131.54, 131.05, 130.95, 129.06, 128.97, 128.45, 125.57, 123.84, 120.28, 118.54 × 2, 117.76, 116.51, 116.36 × 2. TOF MS ES⁺ (*m/z*): [M + H]⁺, calcd for C₂₂H₁₅Br₂FN₄O₃S: 591.9216, found: 592.9294.

N-((6-Bromo-4-((4-bromophenyl)amino)quinolin-3-yl)carbamoyl)-4-chlorobenzenesulfonamide (**21b**). A pale white solid; Yield: 42.6%; m.p.: 284.1–285.4 °C; ¹H-NMR (400 MHz, DMSO-*d*₆) δ (ppm): 11.88 (s, 1H), 8.79 (s, 1H), 8.60 (s, 1H), 8.18 (d, *J* = 12.0 Hz, 4H), 8.03 (s, 1H), 7.94 (d, *J* = 8.2 Hz, 1H), 7.93–7.90 (m, 2H), 7.45 (s, 1H), 7.26 (d, *J* = 8.5 Hz, 2H), 6.44 (s, 1H). ¹³C-NMR (400 MHz, DMSO-*d*₆) δ 144.63, 138.07, 134.75, 132.89, 132.46, 131.54 × 2, 131.34, 131.05, 129.56, 129.07 × 2, 128.04, 127.62 × 2, 127.02, 123.39, 122.07, 119.82, 118.96, 116.03 × 2. TOF MS ES⁺ (*m/z*): [M + H]⁺, calcd for C₂₂H₁₅Br₂ClN₄O₃S: 607.8920, found: 608.8998.

N-((6-Bromo-4-((4-bromophenyl)amino)quinolin-3-yl)carbamoyl)-4-methylbenzenesulfonamide (**21c**). A pale white solid; Yield: 41.9%; m.p.: 279.6–280.2 °C; ¹H-NMR (400 MHz, DMSO-*d*₆) δ (ppm): 12.01 (s, 1H), 8.92 (s, 1H), 8.76 (d, *J* = 11.1 Hz, 4H), 8.13 (s, 1H), 7.94 (s, 2H), 7.74 (d, *J* = 8.3 Hz, 1H), 7.49 (d, *J* = 7.8 Hz, 3H), 7.25 (s, 1H), 6.58 (s, 1H), 2.49 (s, 3H). ¹³C-NMR (400 MHz, DMSO-*d*₆) δ 144.71, 144.21, 141.87, 141.46, 138.11, 132.89, 131.55 × 2, 131.41, 131.07, 129.30 × 2, 128.08, 126.99, 125.64 × 2, 123.37, 120.88, 119.82, 116.00 × 2, 108.86, 20.91. TOF MS ES⁺ (*m/z*): [M + H]⁺, calcd for C₂₃H₁₈Br₂N₄O₃S: 587.9466, found: 588.9545.

N-((6-Bromo-4-((4-bromophenyl)amino)quinolin-3-yl)carbamoyl)-4-(*tert*-butyl)benzenesulfonamide (**21d**). A pale white solid; Yield: 39.3%; m.p.: 259.4–260.3 °C; ¹H-NMR (400 MHz, DMSO-*d*₆) δ (ppm): δ 11.88 (s, 1H), 8.68 (s, 2H), 8.60 (s, 1H), 8.18 (d, *J* = 12.0 Hz, 3H), 8.03 (s, 1H), 7.26 (d, *J* = 8.5 Hz, 2H), 7.18–7.09 (m, 4H), 6.44 (s, 1H), 1.63 (s, 9H). ¹³C-NMR (400 MHz, DMSO-*d*₆) δ 155.20, 145.17, 144.65, 141.80, 141.03, 138.58, 133.35, 132.00 × 2, 131.88, 131.54, 128.53, 127.44, 126.18 × 2, 125.98 × 2, 123.80, 121.28, 120.28, 116.43 × 2, 109.28, 35.23, 31.32 × 2. TOF MS ES⁺ (*m/z*): [M + H]⁺, calcd for C₂₆H₂₄Br₂N₄O₃S: 629.9936, found: 631.0014.

N-((6-Bromo-4-((3-chloro-4-fluorophenyl)amino)quinolin-3-yl)carbamoyl)-4-fluorobenzenesulfonamide (**22a**). A pale white solid; Yield: 46.5%; m.p.: 295.1–296.3 °C; ¹H-NMR (400 MHz, DMSO-*d*₆) δ (ppm): 11.87 (s, 1H), 8.34 (s, 1H), 7.81 (d, *J* = 5.8 Hz, 1H), 7.77–7.59 (m, 2H), 7.50 (d, *J* = 8.5 Hz, 2H), 7.18 (q, *J* = 9.1 Hz, 2H), 7.01 (dd, *J* = 18.2, 8.8 Hz, 2H), 6.95–6.90 (m, 1H), 6.04 (d, *J* = 2.2 Hz, 1H). ¹³C-NMR (400 MHz, DMSO-*d*₆) δ 156.47, 153.39, 142.65, 134.77 × 2, 132.51 × 2, 132.10, 131.50 × 2, 130.15, 129.56 × 2, 128.44, 122.37, 122.01 × 2, 120.65, 119.02, 118.15, 117.92, 115.98. TOF MS ES⁺ (*m/z*): [M + H]⁺, calcd for C₂₂H₁₄BrClF₂N₄O₃S: 565.9627, found: 566.9705.

N-((6-Bromo-4-((3-chloro-4-fluorophenyl)amino)quinolin-3-yl)carbamoyl)-4-chlorobenzenesulfonamide (**22b**). A pale white solid; Yield: 42.6%; m.p.: 282.3–283.7 °C; ¹H-NMR (400 MHz, DMSO-*d*₆) δ (ppm): 11.91 (s, 1H), 10.48 (s, 1H), 7.84 (d, *J* = 8.0 Hz, 3H), 7.76 (d, *J* = 7.5 Hz, 2H), 7.68 (d, *J* = 8.3 Hz, 1H), 7.60 (dd, *J* = 18.5, 10.8 Hz, 2H), 7.54 (d, *J* = 7.9 Hz, 2H), 7.28 (d, *J* = 9.1 Hz, 1H), 6.29 (s, 1H). ¹³C-NMR (400 MHz, DMSO-*d*₆) δ 153.83, 143.10, 135.27, 132.96, 132.55, 131.93 × 2, 130.58, 130.50, 130.01, 129.51, 128.89, 128.13 × 2, 128.08, 127.96, 122.86, 122.46, 119.46, 118.59, 118.37, 116.45. TOF MS ES⁺ (*m/z*): [M + H]⁺, calcd for C₂₂H₁₄BrCl₂FN₄O₃S: 581.9331, found: 582.9409.

N-((6-Bromo-4-((3-chloro-4-fluorophenyl)amino)quinolin-3-yl)carbamoyl)-4-methylbenzenesulfonamide (**22c**). A pale white solid; Yield: 43.2%; m.p.: 278.7–279.9 °C; ¹H-NMR (400 MHz, DMSO-*d*₆) δ (ppm): 11.77 (s, 1H), 10.34 (s, 1H), 7.69 (d, *J* = 8.0 Hz, 3H), 7.61 (d, *J* = 7.5 Hz, 2H), 7.54 (d, *J* = 8.3 Hz, 1H), 7.46

(d, $J = 7.7$ Hz, 2H), 7.39 (d, $J = 7.9$ Hz, 2H), 7.13 (d, $J = 9.1$ Hz, 1H), 6.14 (s, 1H), 2.68 (s, 3H). ^{13}C -NMR (400 MHz, DMSO- d_6) δ 153.84, 143.08 \times 2, 135.23 \times 2, 132.96 \times 2, 131.95 \times 2, 130.62, 130.54, 130.04 \times 2, 128.90, 122.81, 122.45, 121.10, 120.91, 119.48, 118.61, 118.39, 116.43, 21.4. TOF MS ES⁺ (m/z): [M + H]⁺, calcd for C₂₃H₁₇BrClFN₄O₃S: 561.9877, found: 562.9956.

N-((6-Bromo-4-((3-chloro-4-fluorophenyl)amino)quinolin-3-yl)carbamoyl)-4-(*tert*-butyl)benzenesulfonamide (**22d**). A pale white solid; Yield: 38.7%; m.p.: 290.1–291.6 °C; ^1H -NMR (400 MHz, DMSO- d_6) δ (ppm): 11.83 (s, 1H), 10.40 (s, 1H), 7.90 (d, $J = 7.3$ Hz, 3H), 7.75 (d, $J = 8.0$ Hz, 3H), 7.67 (d, $J = 7.5$ Hz, 2H), 7.52 (d, $J = 7.7$ Hz, 1H), 7.45 (d, $J = 7.9$ Hz, 1H), 6.66 (s, 1H), 2.65 (s, 3H), 1.86 (s, 9H). ^{13}C -NMR (400 MHz, DMSO- d_6) δ 153.85, 143.08, 135.23, 132.96, 132.51, 131.95, 130.62, 128.41, 128.01 \times 3, 122.82, 122.46, 121.5 \times 2, 119.49, 118.61 \times 2, 118.39 \times 2, 116.43, 34.3, 31.4 \times 3. TOF MS ES⁺ (m/z): [M + H]⁺, calcd for C₂₆H₂₃BrClFN₄O₃S: 604.0347, found: 605.0425.

4-Chloro-*N*-((6-methoxy-4-((4-methoxyphenyl)amino)-2-methylquinolin-3-yl)carbamoyl)benzenesulfonamide (**23a**). A pale white solid; Yield: 42.6%; m.p.: 290.8–291.2 °C; ^1H -NMR (400 MHz, DMSO- d_6) δ (ppm): 11.86 (s, 1H), 8.31 (d, $J = 10.8$ Hz, 2H), 8.25 (s, 1H), 7.98 (d, $J = 9.2$ Hz, 1H), 7.78 (d, $J = 8.5$ Hz, 1H), 7.67 (d, $J = 8.8$ Hz, 2H), 7.55 (d, $J = 8.4$ Hz, 1H), 7.35 (t, $J = 10.7$ Hz, 2H), 7.33–7.16 (m, 2H), 6.44 (s, 1H), 4.04 (s, 3H), 3.58 (s, 3H), 2.83 (s, 3H), ^{13}C -NMR (400 MHz, DMSO- d_6) δ 154.08, 153.92, 152.32, 148.63, 139.21, 138.67, 138.05, 137.56, 129.21 \times 2, 128.87 \times 2, 128.55, 127.21, 121.98 \times 2, 121.08, 118.98, 117.23, 115.18 \times 2, 97.86, 54.77 \times 2, 20.05. TOF MS ES⁺ (m/z): [M + H]⁺, calcd for C₂₅H₂₃ClN₄O₅S: 526.1078, found: 527.1156.

4-(*tert*-Butyl)-*N*-((6-methoxy-4-((4-methoxyphenyl)amino)-2-methylquinolin-3-yl)carbamoyl)benzenesulfonamide (**23b**). A pale white solid; Yield: 52.6%; m.p.: 291.2–292.7 °C; ^1H -NMR (400 MHz, DMSO- d_6) δ (ppm): 11.75 (d, $J = 3.7$ Hz, 1H), 7.89 (dd, $J = 9.0, 6.4$ Hz, 1H), 7.78 (d, $J = 9.2$ Hz, 2H), 7.62–7.53 (m, 2H), 7.47–7.40 (m, 2H), 7.33 (d, $J = 8.2$ Hz, 2H), 7.24 (s, 2H), 7.23–7.16 (m, 1H), 6.30 (s, 1H), 3.94 (s, 3H), 3.47 (s, 3H), 2.74 (d, $J = 4.0$ Hz, 3H), 1.55 (s, 9H), ^{13}C -NMR (400 MHz, DMSO- d_6) δ 156.28, 154.11, 153.94, 153.23, 148.73, 138.07, 137.94, 137.34, 130.28, 128.53 \times 2, 127.00, 124.86 \times 2, 121.9 \times 2, 121.30, 119.02, 118.12, 114.99 \times 2, 98.72, 54.74 \times 2, 37.18, 28.63 \times 3, 20.74. TOF MS ES⁺ (m/z): [M + H]⁺, calcd for C₂₉H₃₂N₄O₅S: 548.2093, found: 549.2172.

N-((4-((4-Bromophenyl)amino)-6-methoxy-2-methylquinolin-3-yl)carbamoyl)-4-fluorobenzenesulfonamide (**23c**). A pale white solid; Yield: 40.3%; m.p.: 356.1–357.3 °C; ^1H -NMR (400 MHz, DMSO- d_6) δ (ppm): 11.83 (s, 1H), 7.93 (d, $J = 8.4$ Hz, 3H), 7.81 (d, $J = 8.4$ Hz, 2H), 7.32 (d, $J = 9.4$ Hz, 3H), 7.22 (dd, $J = 9.2, 2.7$ Hz, 2H), 7.07 (dd, $J = 9.0, 2.5$ Hz, 1H), 7.00 (d, $J = 2.4$ Hz, 1H), 6.29 (d, $J = 2.5$ Hz, 1H), 3.76 (s, 3H), 2.71 (s, 3H). ^{13}C -NMR (400 MHz, DMSO- d_6) δ 159.82, 155.81, 153.97, 152.07, 140.16, 139.41, 136.48, 132.45 \times 2, 130.61, 130.44 \times 2, 128.60, 127.75, 120.61, 118.52 \times 2, 118.16, 114.79 \times 2, 114.72, 98.94, 55.67, 20.15. TOF MS ES⁺ (m/z): [M + H]⁺, calcd for C₂₄H₂₀BrFN₄O₄S: 558.0373, found: 559.0451.

N-((4-((3-Chloro-4-fluorophenyl)amino)-6-methoxy-2-methylquinolin-3-yl)carbamoyl)-4-fluorobenzenesulfonamide (**23d**). A pale white solid; Yield: 39.5%; m.p.: 285.3–286.1 °C; ^1H -NMR (400 MHz, DMSO- d_6) δ (ppm): 11.87 (s, 1H), 8.34 (s, 1H), 7.81 (d, $J = 5.8$ Hz, 1H), 7.77–7.59 (m, 2H), 7.50 (d, $J = 8.5$ Hz, 2H), 7.40 (s, 1H), 7.18 (q, $J = 9.1$ Hz, 2H), 7.01 (dd, $J = 18.2, 8.8$ Hz, 1H), 6.96–6.88 (m, 1H), 6.04 (d, $J = 2.2$ Hz, 1H), 3.23 (s, 3H), 2.26 (s, 3H), ^{13}C -NMR (400 MHz, DMSO- d_6) δ 156.33, 154.04, 140.82, 140.04, 135.10, 133.00, 131.80, 131.42, 129.37 \times 2, 128.67, 128.23, 121.34, 120.85, 118.87 \times 2, 118.56, 117.05, 115.91 \times 2, 115.01, 99.35, 54.95, 20.73. TOF MS ES⁺ (m/z): [M + H]⁺, calcd for C₂₄H₁₉ClF₂N₄O₄S: 532.0784, found: 533.0862.

^1H -NMR spectra of all the target compounds, ^{13}C -NMR spectra of representative target compounds (**19a**, **19c**, **20c**, **21b**, **21c**, **21d** and **22b**) and TOF-MS spectra of representative target compounds (**19a**, **19c**, **22b** and **23b**) can be seen in the Supplementary Materials.

3.3. PI3K α Kinase Assay

The potent compounds **19a** and **23b** were tested for their activities against PI3K α enzyme using Kinase-Glo Luminescent Kinase Assay (Promega, Madison, WI, USA), with NVPBEZ-235 and PI101 as positive control. The kinase reaction was done in a 384-well black plate. Each well was loaded with 50 μ L of test items (in 90% DMSO) and 5 μ L reaction buffer containing 10 μ g/mL PI substrate (L- α -phosphatidylinositol); Avanti Polar Lipids (Avanti Polar Lipids, Inc., Alabaster, AL, USA); prepared in 3% octyl-glucoside) and the PI3K α protein 10 nM was then added to it. The reaction was started by the addition of 5 μ L of 1 μ M ATP prepared in the reaction buffer (50 mM HEPES pH 7.5, 1 mM EGTA, 3 mM MnCl₂, 10 mM MgCl₂, 2 mM DTT and 0.01% Tween-20) and was incubated for 60 min. It was terminated by the addition of 10 μ L Kinase-Glo buffer. The plates were then read in Synergy 2 readers (BioTek, Winooski, VT, USA) for luminescence detection. The assay was repeated two times and the results expressed as IC₅₀ (inhibitory concentration 50%) were the averages of two determinations.

3.4. mTOR Kinase Assay

The potent compounds **19a** and **23b** were tested for their activities against mTOR enzyme using Kinase-Glo Luminescent Kinase Assay (Promega, Madison, WI, USA), with NVPBEZ-235 and PI101 as positive control. The kinase reaction was done in a 384-well black plate. Each well was loaded with 50 μ L of test items (in 90% DMSO) and 5 μ L reaction buffer containing 10 μ g/mL PI substrate (L- α -phosphatidylinositol); Avanti Polar Lipids (Avanti Polar Lipids, Inc., Alabaster, AL, USA); prepared in 3% octyl-glucoside) and the mTOR protein 2.5 nM was then added to it. The reaction was started by the addition of 5 μ L of 10 μ M ATP prepared in the reaction buffer (50 mM HEPES pH 7.5, 1 mM EGTA, 3 mM MnCl₂, 10 mM MgCl₂, 2 mM DTT and 0.01% Tween-20) and was incubated for 60 min. It was terminated by the addition of 10 μ L Kinase-Glo buffer. The plates were then read in Synergy 2 readers (BioTek, Winooski, VT, USA) for luminescence detection. The assay was repeated two times and the results expressed as IC₅₀ (inhibitory concentration 50%) were the averages of two determinations.

3.5. Cytotoxicity Assay In Vitro

The in vitro cytotoxic activities of all compounds **19a–d**, **20a–d**, **21a–d**, **22a–d** and **23a–d** were evaluated with HepG-2, A549, PC-3 and MCF-7 cell lines by the standard MTT assay, with NVPBEZ235 and Sorafenib as positive control. The cancer cell lines were cultured in minimum essential medium (MEM) supplement with 10% fetal bovine serum (FBS). Approximately 4×10^3 cells, suspended in MEM medium, were plated onto each well of a 96-well plate and incubated in 5% CO₂ at 37 °C for 24 h. The test compounds at indicated final concentrations were added to the culture medium and the cell cultures were continued for 72 h. Fresh MTT was added to each well at a terminal concentration of 5 μ g/mL and incubated with cells at 37 °C for 4 h. The formazan crystals were dissolved in 100 μ L DMSO each well, and the absorbency at 492 nm (for absorbance of MTT formalin) and 630 nm (for the reference wavelength) was measured with an ELISA reader. All of the compounds were tested three times in each of the cell lines. The results were expressed as inhibition rates or IC₅₀ (half-maximal inhibitory concentration) were the averages of two determinations and calculated by using the Bacus Laboratories Inc. Slide Scanner (Bliss) software (the Bacus Laboratories Inc. Slide Scanner (BLISS) system, Lombard, IL, USA).

3.6. Docking Studies

Molecular docking simulation studies were carried out by the AutoDock 4.2 software (The Scripps Research Institute, USA). The docking tutorial we used and the detailed AutoDock basic operational methods can be found at: <http://autodock.scripps.edu/faqs-help/tutorial>. The protein preparation process of flexible docking mainly includes fixing the exact residues, adding hydrogen atoms, removing

irrelevant water molecules, adding charges, etc. The potent compounds were selected as ligand examples, and the structures of PI3K γ (PDB code: 3L08, <http://www.pdb.org/>) were selected as the docking models. Only the best-scoring ligand–protein complexes were used for the binding site analyses. All the docking results were processed and modified in Open-Source PyMOL 1.8. x software (<https://pymol.org>).

4. Conclusions

In summary, five series of phenylsulfonylurea derivatives, **19a–d**, **20a–d**, **21a–d**, **22a–d** and **23a–d**, bearing 4-phenylaminoquinoline scaffolds were designed and synthesized. In addition, we evaluated them for antitumor activity against four cancer cell lines and both PI3K α kinase and mTOR kinase activity (only compounds **19a** and **23b**) in vitro. The pharmacological results indicated that most of the compounds showed moderate cytotoxicity activity against the four cancer cell lines. In particular, the cellular activity of the potent compounds **19a** and **23b** against MCF-7 cell was equal to the positive control Sorafenib, with the IC₅₀ value of 2.88 ± 0.58 and 6.55 ± 0.81 , respectively. Structure–activity relationships (SARs) indicated that the introduction of the methoxyl scaffold into 4-anilinoquinoline scaffold was more favorable than the introduction of halogen to the cellular activity. In general, the methoxy substitution and halogen substitution at 6-position of the quinoline ring played no significant impact on the activity. The para-methoxyl substitution of 4-anilino moiety and para-halogen substitution of phenylsulfonylurea have different impacts on different series of compounds. Moreover, the oxygen atom of phenylsulfonylurea structure can form a hydrogen bond with the residue LYS833 of PI3K γ protein. Further studies will be carried out in the near future.

Supplementary Materials: The Supplementary Materials are available online at <http://www.mdpi.com/1420-3049/23/7/1553/s1>.

Author Contributions: W.Z., S.X. and Z.Y. conceived and designed the experiments; C.W., B.Z. and F.L. performed the experiments; W.L. ran the bioassay evaluation and statistics analysis; and B.Z. started the project and wrote the paper.

Funding: We gratefully acknowledge the generous support provided by The National Natural Science Funds (No. 81460527); The Project Supported by Natural Science Foundation of Jiangxi, China (20171BAB215073 and 20171BAB205101); Natural Science Funds for Distinguished Young Scholar of Jiangxi Province, China (20171BCB23078); Key projects of the youth fund, Natural Science Funds of Jiangxi Province (20171ACB21052); and Jiangxi Provincial Key Laboratory of Drug Design and Evaluation (20171BCD40015).

Conflicts of Interest: The authors declare no conflict of interest.

References

1. Li, B.; Sun, A.; Jiang, W.; Thrasher, J.B.; Terranova, P. PI-3 kinase p110 β : A therapeutic target in advanced prostate cancers. *Am. J. Clin. Exp. Urol.* **2014**, *2*, 188–198. [[PubMed](#)]
2. Liu, P.; Cheng, H.; Roberts, T.M.; Zhao, J.J. Targeting the phosphoinositide 3-kinase pathway in cancer. *Nat. Rev. Drug Discov.* **2009**, *8*, 627–644. [[CrossRef](#)] [[PubMed](#)]
3. Leever, S.J.; Vanhaesebroeck, B.; Waterfield, M.D. Signalling through phosphoinositide 3-kinases: The lipids take centre stage. *Curr. Opin. Cell Biol.* **1999**, *11*, 219–225. [[CrossRef](#)]
4. Giordanetto, F.; Wallberg, A.; Ghosal, S.; Iliefski, T.; Cassel, J.; Yuan, Z.Q.; Wachenfeldt, v.H.; Andersen, S.M.; Inghardt, T.; Tunek, A. Discovery of phosphoinositide 3-kinases (PI3K) p110 β isoform inhibitor 4-[2-hydroxyethyl(1-naphthylmethyl)amino]-6-[(2S)-2-methylmorpholin-4-yl]-1H-pyrimidin-2-one, an effective antithrombotic agent without associated bleeding and insulin resistance. *Bioorg. Med. Chem. Lett.* **2012**, *22*, 6671–6676. [[CrossRef](#)] [[PubMed](#)]
5. Certal, V.; Halley, F.; Vironeoddos, A.; Delorme, C.; Karlsson, A.; Rak, A.; Thompson, F.; Filocherommé, B.; Elahmad, Y.; Carry, J.C. Discovery and optimization of new benzimidazole- and benzoxazole-pyrimidone selective PI3K β inhibitors for the treatment of phosphatase and TENsin homologue (PTEN)-deficient cancers. *J. Med. Chem.* **2012**, *55*, 4788–4805. [[CrossRef](#)] [[PubMed](#)]
6. Hennessy, B.T.; Smith, D.L.; Ram, P.T.; Lu, Y.; Mills, G.B. Exploiting the PI3K/AKT pathway for cancer drug discovery. *Nat. Rev. Drug Discov.* **2005**, *4*, 988–1004. [[CrossRef](#)] [[PubMed](#)]

7. Lv, X.; Ma, X.; Hu, Y. Furthering the design and the discovery of small molecule ATP-competitive mTOR inhibitors as an effective cancer treatment. *Expert Opin. Drug Dis.* **2013**, *8*, 991–1012. [[CrossRef](#)] [[PubMed](#)]
8. Peng, W.; Tu, Z.C.; Long, Z.J.; Liu, Q.; Lu, G. Discovery of 2-(2-aminopyrimidin-5-yl)-4-morpholino-N-(pyridin-3-yl)quinazolin-7-amines as novel PI3K/mTOR inhibitors and anticancer agents. *Eur. J. Med. Chem.* **2015**, *108*, 644–654. [[CrossRef](#)] [[PubMed](#)]
9. Smith, M.C.; Mader, M.M.; Cook, J.A.; Iversen, P.; Ajamie, R.; Perkins, E.; Bloem, L.; Yip, Y.Y.; Barda, D.A.; Waid, P.P. Characterization of LY3023414, a novel PI3K/mTOR dual inhibitor eliciting transient target modulation to impede tumor growth. *Mol. Cancer Ther.* **2016**, *15*, 2344–2356. [[CrossRef](#)] [[PubMed](#)]
10. Asati, V.; Mahapatra, D.K.; Bharti, S.K. PI3K/Akt/mTOR and Ras/Raf/MEK/ERK signaling pathways inhibitors as anticancer agents: Structural and pharmacological perspectives. *Eur. J. Med. Chem.* **2016**, *109*, 314–341. [[CrossRef](#)] [[PubMed](#)]
11. Serra, V.; Markman, B.M.; Eichhorn, P.; Valero, V.; Guzman, M.; Botero, M.; Llonch, E.; Atzori, F.; Di-Cosimo, S.; Maira, M. NVP-BEZ235, a dual PI3K/mTOR inhibitor, prevents PI3K signaling and inhibits the growth of cancer cells with activating PI3K mutations. *Cancer Res.* **2008**, *68*, 8022–8030. [[CrossRef](#)] [[PubMed](#)]
12. Knight, S.D.; Adams, N.D.; Burgess, J.L.; Chaudhari, A.M.; Darcy, M.G.; Donatelli, C.A.; Luengo, J.I.; Newlander, K.A.; Parrish, C.A.; Ridgers, L.H. Discovery of GSK2126458, a highly potent inhibitor of PI3K and the mammalian target of rapamycin. *ACS Med. Chem. Lett.* **2010**, *1*, 39–43. [[CrossRef](#)] [[PubMed](#)]
13. Sutherlin, D.P.; Bao, L.; Berry, M.; Castanedo, G.; Chuckowree, I.; Dotson, J.; Folks, A.; Friedman, L.; Goldsmith, R.; Gunzner, J. Discovery of a potent, selective, and orally available class I phosphatidylinositol 3-kinase (PI3K)/mammalian target of rapamycin (mTOR) kinase inhibitor (GDC-0980) for the treatment of cancer. *J. Med. Chem.* **2011**, *54*, 7579–7587. [[CrossRef](#)] [[PubMed](#)]
14. Venkatesan, A.M.; Dehnhardt, C.M.; Delos, S.E.; Chen, Z.; Dos, S.O.; Ayralkaloustian, S.; Khafizova, G.; Brooijmans, N.; Mallon, R.; Hollander, I. Bis(morpholino-1,3,5-triazine) derivatives: Potent adenosine 5'-triphosphate competitive phosphatidylinositol-3-kinase/mammalian target of rapamycin inhibitors: Discovery of compound 26 (PKI-587), a highly efficacious dual inhibitor. *J. Med. Chem.* **2010**, *53*, 2636–2645. [[CrossRef](#)] [[PubMed](#)]
15. Chang, K.Y.; Tsai, S.Y.; Wu, C.M.; Yen, C.J.; Chuang, B.F.; Chang, J.Y. Novel phosphoinositide 3-kinase/mTOR dual inhibitor, NVP-BGT226, displays potent growth-inhibitory activity against human head and neck cancer cells in vitro and in vivo. *Clin. Cancer Res.* **2011**, *17*, 7116–7126. [[CrossRef](#)] [[PubMed](#)]
16. Cheng, H.; Bagrodia, S.; Bailey, S.; Edwards, M.; Hoffman, J.; Hu, Q.; Kania, R.; Knighton, D.R.; Marx, M.A.; Ninkovic, S. Discovery of the highly potent PI3K/mTOR dual inhibitor PF-04691502 through structure based drug design. *Med. Chem. Commun.* **2010**, *1*, 139–144. [[CrossRef](#)]
17. Xi, L.; Zhang, J.Q.; Liu, Z.C.; Zhang, J.H.; Yan, J.F.; Jin, Y.; Lin, J. Novel 5-anilinoquinazoline-8-nitro derivatives as inhibitors of VEGFR-2 tyrosine kinase: Synthesis, biological evaluation and molecular docking. *Org. Biomol. Chem.* **2013**, *11*, 4367–4378. [[CrossRef](#)] [[PubMed](#)]
18. Hoegenauer, K.; Soldermann, N.; Stauffer, F.; Furet, P.; Graveleau, N.; Smith, A.B.; Hebach, C.; Hollingworth, G.J.; Lewis, I.; Gutmann, S. Discovery and pharmacological characterization of novel quinazoline-based PI3K delta-selective inhibitors. *ACS Med. Chem. Lett.* **2016**, *7*, 762–767. [[CrossRef](#)] [[PubMed](#)]
19. Yadav, R.R.; Guru, S.K.; Joshi, P.; Mahajan, G.; Minto, M.J.; Kumar, V.; Bharate, S.S.; Mondhe, D.M.; Vishwakarma, R.A.; Bhushan, S. 6-Aryl substituted 4-(4-cyanomethyl) phenylamino quinazolines as a new class of isoform-selective PI3K-alpha inhibitors. *Eur. J. Med. Chem.* **2016**, *122*, 731–743. [[CrossRef](#)] [[PubMed](#)]
20. Xin, M.; Hei, Y.Y.; Zhang, H.; Shen, Y.; Zhang, S.Q. Design and synthesis of novel 6-aryl substituted 4-anilinoquinazoline derivatives as potential PI3K δ inhibitors. *Bioorg. Med. Chem. Lett.* **2017**, *27*, 1972–1977. [[CrossRef](#)] [[PubMed](#)]

Sample Availability: Samples of the compounds **19a–d**, **20a–d**, **21a–d**, **22a–d** and **23a–d** are available from the authors.



© 2018 by the authors. Licensee MDPI, Basel, Switzerland. This article is an open access article distributed under the terms and conditions of the Creative Commons Attribution (CC BY) license (<http://creativecommons.org/licenses/by/4.0/>).